CLM-P872

CLM-P872

Transport from Ion Temperature Gradient Driven Turbulence

N. Mattor

CULHAM LABORATORY
LIBRARY
19 JAN 1990
a

R

CULHAM LIBRARY
REFERENCE ONLY

CULHAM
LABORATORY

AEA TECHNOLOGY

This document is intended for publication in a journal or at a conference and is made available on the understanding that extracts or references will not be published prior to publication of the original, without the consent of the authors.

Enquiries about copyright and reproduction should be addressed to the Librarian, UKAEA, Culham Laboratory, Abingdon, Oxon. OX14 3DB, England.

Transport From Ion Temperature Gradient Driven Turbulence

Nathan Mattor
Culham Laboratory, Abingdon, Oxon. OX14 3DB, England
Euratom / UKAEA Fusion Association

and

University of Wisconsin
Madison, Wisconsin 53706

Abstract

The ion thermal conductivity (χ_i) arising from strong ion temperature gradient driven turbulence is derived, taking account of effects from ion resonance damping (linear and nonlinear), and broader radial eigenmodes. It is assumed that when a mode resonates with ions (as determined from a local solution of the gyrokinetic equation), it will saturate at a level too small to contribute significantly to transport. The remaining modes are fluid and strongly turbulent, and a mixing length estimate is used to find χ_i. The results are a prediction of the threshold of strong transport (which is different from the linear stability threshold), and an ion thermal conductivity given approximately by:

$$\chi_i = 0.037 \frac{L_s^2 \rho_i}{L_n^3} \frac{\tau^3}{(1+\tau)^{3/2}} (\eta_i - 1.2)^3 \rho_i^2 \Omega_i,$$

which contains more physical effects basic to the η_i mode than previous estimates of χ_i. A more accurate but more elaborate form of χ_i is supplied in the text.

I. Introduction

In the last decade there have been a number of nonlinear studies of the ion temperature gradient driven instability ("η_i turbulence"). However, as yet no single theory has included enough basic dynamics to determine the associated ion thermal conductivity χ_i to within an order of magnitude. This work is an attempt to bring together previous theories in order to predict χ_i more accurately for all regimes of η_i. The sheared slab model is considered, for which the most detailed nonlinear understanding is available.

To see what physics must go into an accurate prediction of the χ_i from η_i turbulence, consider the following argument. In the fluid strong turbulence regime, the transport associated with a mode increases quite rapidly with the radial modenumber,[1] l (with diffusivity increasing like $(2l+1)^3$), and so χ_i is quite sensitive to whatever effect it is that reverses this trend at high l. For high enough l the modes stabilize linearly, but before this occurs, there are at least two changes in the nonlinear physics that effectively cut off transport. These are the onset of ion Compton scattering (which replaces 3-wave resonances), and the transition from strong to weak turbulence, which do not necessarily occur together. Although these are not well explored for η_i modes at high l, a recent study of the $l = 0$ mode near the instability threshold[2] indicates that the presence of ion Compton scattering holds the fluctuations and transport down to a negligible amount (by a factor of $(L_T/L_s)^2 \ll 1$ compared with fluid turbulence), and it is reasonable to expect a similar diminution for higher l. Weak turbulence (which occurs roughly when $|\gamma| \ll |\omega_r|$) will also hold the transport down by introducing an additional factor of approximately γ/ω_r into the mixing length estimate of χ_i. Thus, transport is determined by the radial eigenmode which is on the boundary between different regimes of nonlinear behaviour (either fluid vs. kinetic saturation, or strong vs. weak turbulence). No previous study has addressed this issue, which leads to the conclusion that no prevoius prediction of χ_i from η_i modes is very accurate.

An accurate prediction of χ_i must take combined account of the effects of ion resonances (linear and nonlinear), strong and weak turbulence, and higher radial eigenmodes. Although a full analytical theory is probably unfeasible, all these effects can at least be accounted for with the aid of three assumptions that incorporate results from previous detailed (but incomplete) analyses. First and most importantly, nonlinear kinetic effects can be incorporated by assuming that whenever *linear* wave-particle resonances are significant for a mode, then *nonlinear* resonances will saturate the instability, and will hold the amplitude to a level too small to contribute to transport (even though the mode may be linearly unstable). This is supported by a recent kinetic weak turbulence study,[2] and here it is additionally assumed that robust damping occurs also for *strong* turbulence with ion resonances. The second assumption is that the frequency of a normal mode is given roughly by the *local* solution to the mode equation, in which ω is solved as a function of $k_{\|}$. In reality, a normal mode will span a range of $k_{\|}$ and have only a single frequency, but this may be obtained by some judiciously selected average of the local frequency over the width of the normal mode. This assumption allows substantial analytical simplification of the problem, and is supported by the success of local approaches[2,6] in light of full normal mode analyses.[1,7] The third assumption is that transport from an η_i mode in the fluid strong turbulence regime is well approximated by the mixing length estimate, $\chi_i = \gamma\Delta_x^2$, chosen at some average wavenumber (although this will not hold for all regimes of the η_i mode). This assumption is supported by a variety of studies of fluid strong turbulence from η_i modes, including dimensional analysis,[3] a two-point renormalized spectral theory,[4] and a diffusion-as-eigenvalue calculation.[5]

With these assumptions, the analysis can proceed as follows. Starting with the kinetic linear dielectric function,[6,8] a local approximation is used to derive the frequency as a function of radius, from which the region of fluid strong turbulence may be assessed. The fluid region is determined by the condition $|\zeta| \equiv |\omega/\sqrt{2}k_{\|}v_i| > 1$, (i.e., the parallel phase velocity is larger than the ion thermal velocity). The strong turbulence region (which is not the same as the fluid region) is determined approximately by the condition $\gamma > 0$, since weak turbulence for the present problem occurs near the limit of linear stabilization. (The definition of the strong turbulence region is rather less certain than that of the fluid region, but fortunately it appears that the latter provides the determining condition except for very large η_i. Furthermore, with the present definition, a mode that is weakly turbulent is close to linear stability, where the associated transport is sure to vanish.) Knowledge of these regions then enables determination of the transport threshold (from the condition that a region of fluid strong turbulence exist), and the ion thermal conductivity (from a mixing length estimate applied to the broadest mode contained within this region). The growth rate necessary for the mixing length estimate is obtained from a normal mode analysis, which obviously may be performed in the fluid limit for the modes of interest.

II. Model and Local Analysis

The equation describing the linear kinetic η_i instability in sheared slab geometry has been derived previously.[6,8] The ions are gyrokinetic, with temperature and density gradients in the radial ($\hat{x}$) directions, the electrons are adiabatic, and the magnetic field is in a sheared slab configuration, with $\vec{B} = B_0\left(\hat{z} + \frac{x}{L_s}\hat{y}\right)$. This yields

$$\epsilon_{\vec{k}}(\omega)\,\tilde{\phi}_{\vec{k}} = 0, \tag{1}$$

where the linear dielectric function is

$$\epsilon_{\vec{k}}(\omega) = \Omega(1+1/\tau) - \eta_i\zeta^2\Gamma_0 + \left[\eta_i\left(\frac{1}{2} + b\left(1 - \frac{\Gamma_1}{\Gamma_0}\right)\right) - 1 - \eta_i\zeta^2 + \Omega\right]\zeta Z(\zeta)\Gamma_0. \tag{2}$$

where,

$$\Omega = \omega/\omega_{*i}, \qquad \omega_{*i} = \frac{k_y\rho_i^2\Omega_i}{L_n}, \qquad \tau = T_e/T_i, \qquad \eta_i = L_n/L_T,$$

$$L_n^{-1} = \frac{d\ln n_0}{dx}, \qquad L_T^{-1} = \frac{d\ln T_{i,0}}{dx}, \qquad \zeta^2 = \frac{\omega^2}{2k_\parallel^2 v_i^2}, \qquad \Gamma_n = e^{-b}I_n(b),$$

$$b = \rho_i^2\left(k_x^2 + k_y^2\right), \qquad \rho_i = v_i/\Omega_i, \qquad \Omega_i = eB/m_i c, \qquad v_i^2 = T_i/m_i,$$

$\omega = \omega_r + i\gamma$ is the linear frequency, $Z(\zeta)$ is the plasma dispersion function, and I_n is the modified Bessel function of order n. For a sheared slab geometry, $k_\parallel = k_y x/L_s$. where x is the distance to the rational surface. The local solution to Eq. (1) is symmetric about $x = 0$, and so consideration is restricted to $x \geq 0$.

The strong turbulence and fluid regions may be described in terms of two positions in x (Fig. 1) which vary as functions of η_i, b, τ, and L_n/L_s. First, the fluid region is demarcated by the Landau damping radius, x_{LD}, defined as the position where $|\zeta| = 1$. For modes contained within x_{LD}, the phase velocity will be larger than the ion thermal velocity, and resonances will not occur. It is important to note that while the condition $|\zeta| > 1$ is only barely satisfied in the local theory, this condition is well satisfied for normal modes within the fluid region, for which ω is constant while $k_{\|} \to 0$ for $x \to 0$. Second, the strong turbulence region is limited approximately by the marginal stability radius, x_m, inside of which $\gamma > 0$ (and vice versa), which has been derived previously[6]. Modes narrower than x_m will be strongly turbulent (with $|\gamma_r| \gtrsim |\omega_r|$ on the average over the mode), while modes that extend beyond x_m will become weakly turbulent and eventually stabilize. The appropriate mixing length is then $x_{ML} = \min(x_m, x_{LD})$, since this is the width of the broadest mode with *both* $|\zeta| > 1$ and $|\gamma| \gtrsim |\omega_r|$.

For a local analysis, it is convenient to eliminate ω and $k_{\|}$ from Eq. (1) in favor of ζ and x, yielding

$$\epsilon_{\vec{k}}(\zeta) = \sqrt{2}\zeta sxp - \eta_i\zeta^2 + \left(\delta - \eta_i\zeta^2 + \sqrt{2}\zeta sx\right)\zeta Z(\zeta) = 0, \tag{3}$$

where the following notation has been introduced:

$$p = \frac{1 + 1/\tau}{\Gamma_0}, \qquad \delta = \frac{\eta_i}{\eta_c} - 1, \qquad \eta_c = \left[\frac{1}{2} + b\left(1 - \frac{\Gamma_1}{\Gamma_0}\right)\right]^{-1},$$

$s = L_n/L_s$, $\zeta = \zeta_r + i\zeta_i$, and x has been normalized to ρ_i. Here η_c is the ($k_\perp$ dependent) critical value[6] of η_i, which follows from the expression for the marginal stability radius x_m, where $\gamma = 0$. This is derived by setting the real and imaginary parts of $\epsilon_{\vec{k}}(\zeta_r)$ to zero at x_m, yielding

$$s^2x_m^2 = \frac{\eta_i\delta}{2p(p-1)}$$

$$\zeta_m^2 = \frac{p\delta}{\eta_i(p-1)}.$$

For $\eta_i > \eta_c$, then $x_m^2 > 0$ and instability can exist. However, near threshold the instability is essentially kinetic, since $|\zeta| < 1$ when $\delta \ll 1$.

The fluid threshold can be found by noting that $|\zeta| = 1$ first at $x = 0$, where Eq. (3) can be written as

$$\frac{\delta}{\eta} = \zeta^2\left(1 + \frac{1}{\zeta Z(\zeta)}\right). \tag{4}$$

Since the right hand side of Eq. (4) must be real, then ζ must be imaginary, and thus at the fluid threshold, $\zeta = i$. The right hand side of Eq. (4) can then be evaluated, leading to a fluid threshold of

$$\eta_c^{\text{fluid}} = \left(\eta_c^{-1} + .319\right)^{-1}.$$

Figure 2 shows η_c^{fluid} and η as functions of b. The minimum value is $\eta_c^{\text{fluid}} \simeq 1.2$ (compare the linear threshold of .9), which occurs at $b \simeq 1$.

To find the Landau damping radius, an expression for $\zeta(x)$ is needed. This is obtained by first finding $\zeta(x=0)$ from perturbing Eq. (4) about $\zeta = i$ for small $\eta_i - \eta_c^{\text{fluid}}$, and then expanding $\zeta(x)$ to second order in a Taylor series and solving Eq. (3). After quite a bit of algebra, this yields

$$|\zeta(x)|^2 = 1 + 12.4\frac{\left(\eta_i - \eta_c^{\text{fluid}}\right)}{\eta_i^2} - 202\frac{(p - .758)^2}{\eta_i^2}s^2x^2. \tag{5}$$

Setting $|\zeta|^2 = 1$ yields the Landau damping radius for $\eta_i \simeq \eta_c^{\text{fluid}}$

$$x_{LD} = .247\frac{\left(\eta_i - \eta_c^{\text{fluid}}\right)^{1/2}}{s(p - .758)}. \tag{6}$$

Unfortunately, the expansions that go into Eq. (5) have a rather narrow range of convergence, and Eqs. (5) and (6) are only valid for η_i very near the fluid threshold (as tested numerically). As η_i increases well above threshold, x_{LD} moves beyond the radius of convergence about $x = 0$. For this regime, x_{LD} may be found by an expansion of $\zeta(x)$ about $x = x_m$. This is done by noting that ζ_i (where $\zeta = \zeta_r + i\zeta_i$) is small near x_m, and so the approximation $\epsilon_r(\zeta_r) = 0$ and $\zeta_i = \frac{-\epsilon_i(\zeta_r)}{\partial\epsilon_r/\partial\zeta_r}$ is applicable. The solution around x_m is then:

$$\zeta_r \simeq \text{constant} = \zeta_m$$
$$\zeta_i \simeq \sqrt{2\pi}\zeta_m\left(1 - \frac{x}{x_m}\right)e^{-\zeta_m^2}$$

Setting $|\zeta|^2 = 1$ yields the Landau damping radius for $\eta_i \gg \eta_c^{\text{fluid}}$

$$x_{LD} = x_m\left(1 - \sqrt{-1 + 1/\zeta_m^2 e^{\zeta_m^2}/\sqrt{2\pi}}\right). \tag{7}$$

When $\zeta_m^2 \geq 1$, the mode is fluid across the entire zone of instability, and so x_m is the correct mixing length. This occurs when

$$\eta_i \geq \left[\frac{1}{p} - .5 + b\left(1 - \frac{\Gamma_1}{\Gamma_0}\right)\right]^{-1}.$$

In Fig. 2 this value is the boundary of the "Unstable and Fluid" region. For low η_i ($\lesssim 4$ for $\tau = 1$), it is x_{LD} that limits the mixing length, while for larger η_i it is x_m.

III. Fluid Normal Modes

The local theory has provided the width of the broadest fluid, strongly turbulent mode. For a mixing length estimate, a relation between the mode width and the growth rate is required. This is obtained through a normal mode analysis, which can be done in the fluid limit since $\zeta \geq 1$ for these modes.

The structure and growth rate of the fluid normal modes is obtained by expanding Eq. (1) to order $(k_x\rho_i)^2$ and $1/\zeta^2$, and taking $k_x^2 \rightarrow -\partial^2/\partial x^2$, which yields the Weber's equation:

$$\frac{\partial^2}{\partial x^2}\tilde{\phi} + \frac{1}{C}\left[A - Bx^2\right]\tilde{\phi} = 0 \tag{8}$$

where

$$A = \Omega\,(p-1) + \frac{\eta_i}{2} - \delta$$

$$B = \frac{s^2}{\Omega^2}\left[\delta + \Omega - \frac{3}{2}\eta_i\right]$$

$$C = \frac{-1}{\Gamma_0}\frac{\partial}{\partial b}\left[\Gamma_0\left(\frac{\eta_i}{2} - \Omega\right) - \Gamma_0\delta\right].$$

The solutions of Eq. (8) are the Hermite functions:

$$\tilde{\phi} = H_l\left(\left(\frac{B}{C}\right)^{\frac{1}{4}} x\right) exp\left(\sqrt{\frac{B}{C}}\frac{x^2}{2}\right), \tag{9}$$

where the dispersion relation is $A = (2l+1)\sqrt{BC}$, and $l = 0, 1, 2\ldots$ is the radial mode number. The mode width is obtained by taking the normalized x^2 moment of $\tilde{\phi}$, yielding

$$\Delta_x^2 = \left(l + \frac{1}{2}\right)\sqrt{C/B}. \tag{10}$$

The present analysis considers only the l that yields $\Delta_x = x_{ML}$, radial quantization may be neglected, thereby approximating l as continuous. Thus, eliminating l between Eq. (10) and the dispersion relation, and setting $\Delta_x = x_{ML}$ yields:

$$[p-1]\,\Omega^3 + [1 - \eta_i/\eta_{flr}]\,\Omega^2 - \left[2s^2x_{ML}^2\right]\Omega + 2s^2x_{ML}^2\,(1 + \eta_i - \eta_i/\eta_{flr}) = 0, \tag{11}$$

where $\eta_{flr} \equiv (b - b\Gamma_1/\Gamma_0)^{-1}$ may be regarded as the point where finite Larmor radius corrections become important. When $\eta_i \ll \eta_{flr}$, one recovers the usual η_i growth rate by balancing the second and fourth terms in Eq. (11), yielding

$$\Omega = i\sqrt{1+\eta_i}\,s x_{ML}, \tag{12}$$

For higher values of η_i or b, then η_i/η_{flr} in Eq. (11) is no longer negligible, and numerical solution is required.

IV. Transport

With the mixing length determined and the growth rate given by Eq. (11), the ion thermal conductivity can now be estimated via $\chi_i(b) = \gamma x_{ML}^2$. In the near threshold regime, Eqs. (6) and (12) yield

$$\chi_i(b) = .015\frac{\rho_i L_s^2}{L_n^3}\frac{k_y\rho_i\Gamma_0^3}{(1-.758\Gamma_0+1/\tau)^3}\left(\frac{1+\eta_i-\eta_i/\eta_{flr}}{1-\eta_i/\eta_{flr}}\right)^{1/2}\left(\eta_i-\eta_c^{\text{fluid}}\right)^{3/2}\rho_i^2\Omega_i. \tag{13}$$

Taking $k_y\rho_i \simeq \sqrt{b}$, then $\chi_i(b)$ is maximized for $b \simeq 1$, which yields

$$\chi_i = .013\frac{\rho_i L_s^2}{L_n^3}\frac{(\eta_i-1.2)^{3/2}}{(1+1.54/\tau)^3}\rho_i^2\Omega_i. \tag{14}$$

The η_i scaling in Eq. (14) covers only a very narrow range above threshold, since terms of higher order in $\eta_i - \eta_c^{\text{fluid}}$ have been neglected in deriving x_{LD}. As η_i increases, the numerical coefficient in Eq. (14) increases, while the scaling with other parameters remains largely unaffected.

In the $\eta_i \gg \eta_c^{\text{fluid}}$ regime, a mixing length estimate using Eqs. (7) and (12) yields

$$\chi_i(b) = \frac{\rho_i L_s^2}{L_n^3}k_y\rho_i\left[\frac{\eta_i\left(\frac{\eta_i}{\eta_c}-1\right)\Gamma_0^2}{(1+1/\tau)(1+1/\tau-\Gamma_0)}\right]^{3/2}\left(\frac{1+\eta_i-\eta_i/\eta_{flr}}{1-\eta_i/\eta_{flr}}\right)^{1/2}$$
$$\times\left(1-\sqrt{2\pi}e^{-\zeta_m^2}\sqrt{-1+1/\zeta_m^2}\right)^3\rho_i^2\Omega_i. \tag{15}$$

The right hand side of Eq. (15) vanishes at low b from the $k_y\rho_i$ coefficient, and is reduced at high b by the η_{flr} terms (numerical solutions of Eq. (11) indicate that these begin to diminish γ for $b \gtrsim 1/\eta_i$). Choosing $b \simeq 1/2\eta_i$ roughly balances these two effects, yielding:

$$\chi_i = \frac{\tau^3}{(1+\tau)^{3/2}}\frac{\rho_i L_s^2}{L_n^3}\eta_i(1+2\eta_i)^{1/2}(\eta_i-\eta_c)^{3/2}\rho_i^2\Omega_i. \tag{16}$$

Equations (14) and (16) represent χ_i at two extremes, but what is needed is a value for χ_i that is valid for *all* η_i. Analytically, this is difficult or impossible to obtain accurately, and so it seems appropriate to use a numerical strategy, as follows. The dependence on $s = L_n/L_s$ is extracted easily by noting that the substitution $sx \rightarrow x'$ in Eqs. (3) and (11) eliminates s from the equations, which may be reinserted at the end to yield $\chi_i \propto 1/s^2$.

The ion thermal conductivity may then be obtained by a mixing length estimate, with x_{ML} from numerical solution to Eq. (3) and γ from inserting this into Eq. (11)). The b dependence is eliminated by maximizing χ_i as a function of b (the resulting b is shown in Fig. 2 for $\tau = 1$). This leaves η_i and τ dependence, which are obtained by hand choosing a form that looks like the numerical solution (using Eqs. (14) and (16) as guidelines) for all regimes in η_i (except $\eta_i < 0$), and in the neighborhod of $\tau = 1$. This produces

$$\chi_i = \frac{L_s^2 \rho_i}{L_n^3} f\left(\eta_i, \tau\right) \rho_i^2 \Omega_i \tag{17}$$

Numerical evaluation of $f\left(\eta_i, \tau\right)$ is shown in Fig. 3, and a reasonable fit is given by:

$$f\left(\eta_i, \tau\right) = \frac{\tau^3}{(1+\tau)^{\frac{3}{2}}} \max\left[0.026\left(\eta_i - 1.2\right)^{3.1+.3\sqrt{\tau}},\ 0.066\sqrt{\tau}\left(\eta_i - \left(1 + 0.6e^{-.09/\tau^2}\right)\right)^3\right], \tag{18}$$

where terms of the form $(\eta_i - \alpha)$ vanish if $\eta_i < \alpha$. Equations (17) and (18) are the principal result of this work. A simpler but less accurate estimate is given in the abstract. There is no restriction on the range of applicability in either η_i or L_n/L_s, although there might be an additional term when $\eta_i < 0$ (where Eq. (18) predicts no transport).

Equation (17) shows improved confinement with increasing T_i/T_e and decreasing L_s (which may be related to increasing current), which compare favorably with experimental observations.[9] The scaling with L_n is ambiguous, since more peaked density profiles (lower L_n) will increase χ_i through the $1/L_n^3$ dependence in Eq. (17), but also decrease χ_i by driving η_i closer to threshold in Eq. (18). This could underlie the seemingly contradictory experimental observations that pellet injection improves confinement by peaking the density, while the very flat density profiles of H-modes seem to show no degraded confinement. Finally, Eq. (17) shows a rather strong dependence on the temperature gradient, with $\chi_i \propto L_T^{-3}$. With this, it is possible that the strong diminution of χ_i towards the edge (from the $T^{-3/2}$ dependence in ρ_i^3) could be overcome by only a mild increase in η_i.

V. Conclusions

This paper has presented a method for including the effects of higher radial eigenmodes, ion Compton scattering, and weak turbulence in the χ_i resulting from η_i turbulence. The important threshold is not the linear stability threshold ($\eta_i \simeq 0.9$), but the threshold of fluid behaviour ($\eta_i \simeq 1.2$). The resulting χ_i, given by Eqs. (17) and (18), is rather different from that calculated by the usual method of considering only the fluid $l = 0$ mode and the linear stability threshold.

The assumptions of this paper, along with the model of a sheared slab geometry with adiabatic electrons, may be regarded as rather crude, but from a physical point of view they are less crude than more rigorous theories or more elaborate models that ignore altogether the effects considered here, which are quite basic to the η_i mode. Thus, it is possible that Eq. (17) could give better agreement with experiments than previous predictions. The calculational technique used here, which is based mainly on a local solution of the gyrokinetic equation, could be applied to a more realistic model, such as one incorporating toroidal effects or unthermalized ion distributions. However, a more rigorous approach would have to address the nonlinear gyrokinetic equation in the limit of strong turbulence, which is perhaps analytically unfeasible; therefore, numerics are probably necessary. It is especially desirable to check the assumptions that ion Compton scattering will reduce the transport in the strong turbulence regime (shown previously only for weak turbulence[2]), and that nonlinear resonances occur along with linear resonances.

Acknowledgements

The author would like to thank Dr. J. W. Connor and Dr. T. Stringer for thoughtful readings of the manuscript, and Dr. O. Gruber and Dr. F. Tibone for helpful comments.

References

1. P. W. Terry et al., Phys. Fluids **31**, 2920 (1988).
2. N. Mattor and P. H. Diamond, to appear in Phys. Fluids B, October, 1989.
3. J. W. Connor, Nucl. Fusion **26**, 193 (1986).
4. G. S. Lee and P. H. Diamond, Phys. Fluids **29**, 3291 (1986).
5. N. Mattor and P. H. Diamond, Phys. Fluids **31**, 1180 (1988).
6. B. B. Kadomtsev and O. P. Pogutse in *Reviews of Plasma Physics*, edited by M. A. Leontovitch (Consultants Bureau, New York, 1970) Vol. 5, pg 249.
7. R. E. Waltz, W. Pfeiffer, and R. R. Dominguez, Nucl. Fusion **20**, 43 (1980).
8. A. A. Galeev, V. N. Oraevskii, and R. Z. Sagdeev, Sov. Phys. JETP **17**, 615 (1963).
9. S. M. Kaye, Phys. Fluids **28**, 2327 (1985).

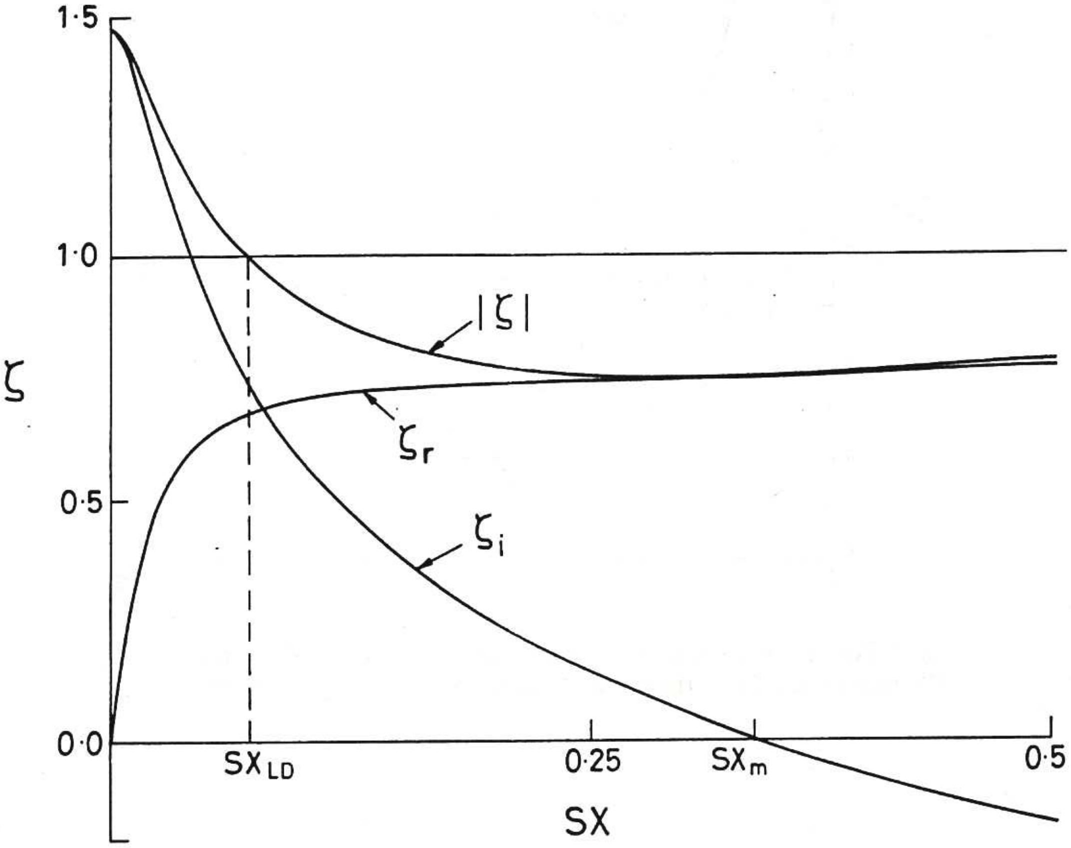

Fig. 1 $\zeta = \omega/\sqrt{2}k_{\parallel}$ as a function of sx, for $\eta_i = 2$, $b = 0.5$, and $\tau = 1$, showing the marginal stability radius, x_m, and the Landau damping radius, x_{LD}.

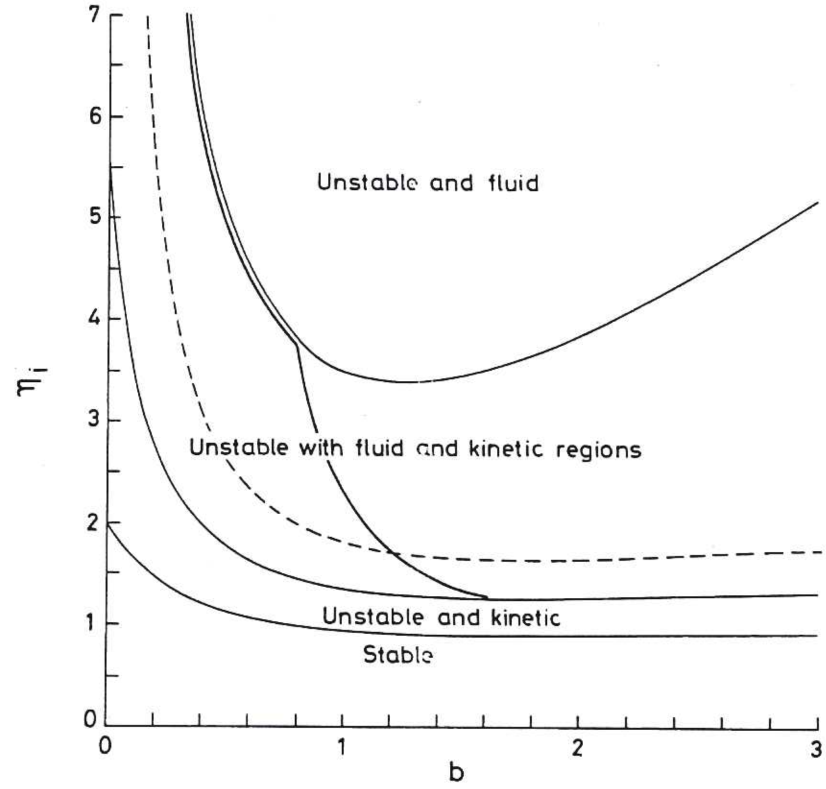

Fig. 2 Zones of behaviour for the local theory. The dotted line represents η_{flr}. The heavy solid line is the b that maximizes χ_i (for $\tau=1$), taken here as b_{rms}.

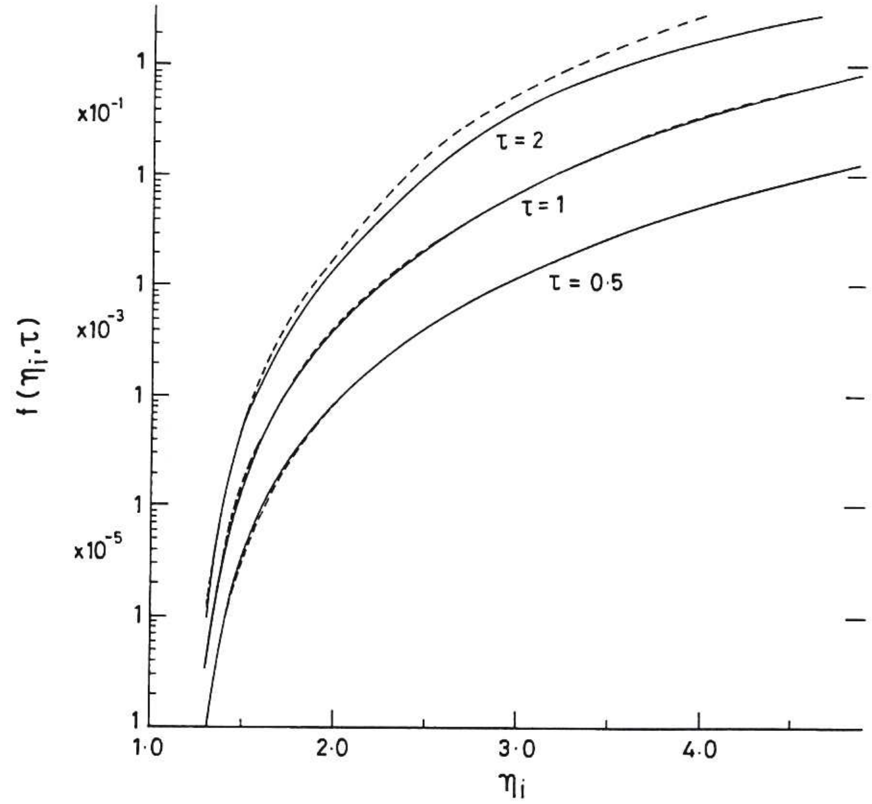

Fig. 3 Numerical $f(\eta_i, \tau)$ used in Eq.(17) (solid lines), shown next to best fit, Eq.(18) (dotted lines).